A Boundary Element Based Methodology for Modeling and Simulation of Lab-on-Chip devices

Indranil Chowdhury, Vikram Jandhyala and John Rockway
Electrical Engineering Bldg., Box 352500, University of Washington,Seattle, WA 98195
Email: {burunc, jandhyala, jrockway}@ee.washington.edu

Abstract

This paper combines lumped circuits, electromagnetic and fluidic models in order to predict dielectrophoretic and fluidic traction forces for biochips. The boundary element method (BEM) is used for solving both electromagnetic (EM) and fluidic domain problems. A coupled circuit-EM methodology is used to model electrical excitations. The resulting simulator accurately predicts the force fields on arbitrarily-shaped bio-species. This integrated computational tool enables the exploration of new design ideas for microfluidic Lab-on-chip devices.

1. Introduction

Novel Lab-on-Chip (LoC) technologies provide automation of faster and cheaper biomedical devices for point-of-care diagnostics [1]. These systems use microfluidic channels along with on-chip electrode arrays in order to accomplish multiple functionalities on a single platform – including transport, concentration, separation and mixing of species or particles of interest. Non-uniform EM fields that are commonly used for particle manipulation include dielectrophoresis (DEP), dielectrophoretic field-flow fractionation (DEP-FFF), and magnetophoresis (MAP). The combination of electromagnetic and fluidic traction forces traps and separates bio-species inside the LoC chamber. Design and automation of such systems require rigorous computational tools for analysis of the various force fields and also due to the interplay across multiple physical domains (as depicted in fig 1). Previous efforts have explored various analytic and numerical techniques like the finite element method [2]. This paper utilizes the boundary element method (BEM), for the analysis of EM as well as fluidic systems. A coupled circuit-electromagnetic formulation is discussed in the first section. In the second section, boundary element formulation for predicting DEP force and the fluid traction forces on the particle are presented. In the last section, simulation examples will be presented to demonstrate the functionalities of the proposed method. The resulting methodology can be used for the analysis of complicated electrode array designs (e.g., interdigitated parallel arrays or polynomial designs), as well as the flow field and traction forces inside an arbitrary channel. Additionally the presented method is amenable to acceleration using rapid iterative $O(N)$ solvers like the fast multipole and multilevel rank-revealing QR algorithms, which provide a critical advantage over the commonly used finite element methods for large computational domains.

2. Coupled circuit-EM formulation

Electric field and magnetic field equations (EFIE and MFIE) are given by [3]:

$$\mathbf{E}^s = -j\omega\mathbf{A} - \nabla\phi - \frac{1}{\varepsilon}\nabla\times\mathbf{F} \text{ , and } \mathbf{H}^s = \frac{1}{\mu}\nabla\times\mathbf{A} - \nabla\psi - j\omega\mathbf{F}$$

The magnetic vector potential ($\mathbf{A}$) and scalar potentials ϕ are expressed in terms of the electric surface current $\mathbf{J}$ by,

$$\mathbf{A}(\mathbf{r}) = \mu\int_S G(\mathbf{r},\mathbf{r}')\mathbf{J}(\mathbf{r}')dS' \text{, and } \phi(\mathbf{r}) = \frac{-1}{j\omega\varepsilon}\int_S G(\mathbf{r},\mathbf{r}')\nabla\cdot\mathbf{J}(\mathbf{r}')dS'$$

The electric vector and scalar potentials are defined in terms of the magnetic surface current $\mathbf{M}$.

$$\mathbf{F}(\mathbf{r}) = \varepsilon\int_s G(\mathbf{r},\mathbf{r}')\mathbf{M}(\mathbf{r})d\mathbf{S} \text{, and } \psi(\mathbf{r}) = \frac{-1}{j\omega\mu}\int_s G(\mathbf{r},\mathbf{r}')\nabla\cdot\mathbf{M}(\mathbf{r})d\mathbf{S}$$

$G(\mathbf{r},\mathbf{r}') = e^{-jk|\mathbf{r}-\mathbf{r}'|}/4\pi|\mathbf{r}-\mathbf{r}'|$ is the Green's function in the corresponding region. The boundary conditions are obtained by equating the tangential fields from each region. Next, the circuit part is connected to the surface currents by enforcing a modified current-continuity equation,

$$\nabla \cdot \mathbf{J} + j\omega\rho = \begin{cases} I_c, & \mathbf{r} \in S_C \\ 0, & \text{otherwise} \end{cases}$$

where I_C is the current injected from the circuit contact, and S_C is portion of the discretized metal surface connected directly to the circuit nodes. The scalar potentials are tied to the circuit node voltage V_n, by the following Kirchoff's Voltage Law (KVL) expression: $\phi(\nabla \cdot \mathbf{J}) + \phi(I_C) = V_n$. The contact current is connected to the circuit by including an additional term I_C in the Kirchoff's Current Law (KCL) equation associated with circuit node n as, $I_c = MNA(I_n)$, where MNA is the modified nodal analysis block matrix that represents the circuit part of the system. The combined system of equations is solved by the method of moments (MoM) technique, and allows the control of the EM section by lumped circuit elements.

3. BEM formulation for DEP and Stokes flow

The approach presented here relies on computation of the surface charge densities induced by the incident EM fields that are in turn produced by the circuit sources. The induced charges are then used to compute the total DEP force on the particle. Consider an arbitrary particle bounded by a surface S. The continuity of the scalar potential across S is given by [4],

$$-\int_S ds \int_S G_s(\mathbf{r}, \mathbf{r}')\, \sigma_s\, ds' + \int_S ds \int_S G_i(\mathbf{r}, \mathbf{r}')\, \sigma_i\, ds' = \int_S \phi_e^{inc}\, ds - \int_S \phi_i^{inc}\, ds$$

where the subscripts i and e represent the interior and the exterior of the object and σ is the unknown equivalent surface charge density. Taking the gradients of the potential leads to the computation of the electric flux density, the normal component of which is continuous across the particle surface:

$$\hat{\mathbf{n}} \cdot \varepsilon_e \int_S ds \ \ \nabla \int_S G_e(\mathbf{r}, \mathbf{r}')\, \sigma_e\, ds' - \hat{\mathbf{n}} \cdot \varepsilon_i \int_S ds \ \ \nabla \int_S G_i(\mathbf{r}, \mathbf{r}')\, \sigma_i\, ds' = \hat{\mathbf{n}} \cdot \varepsilon_e \int_S ds \mathbf{E}_e^{inc} - \hat{\mathbf{n}} \cdot \varepsilon_i \int_S ds \mathbf{E}_i^{inc}$$

where $\hat{\mathbf{n}}$ is the unit normal of the surface S pointing in the outward direction. Upon discretization of the particle surface the above system of equations form a complete set of linear equations, the solution of which yields the equivalent charge densities. The total DEP force acting on the object can then be found as

$$\mathbf{F} = -\int_S \sigma_e(\mathbf{r}) ds \nabla \int_S G_e(\mathbf{r}, \mathbf{r}') \sigma_e(\mathbf{r}') ds' + \int_S ds\, \sigma_e(\mathbf{r}) \mathbf{E}_e^{inc}$$

Microfluidics systems are characterized by laminar flow, where the flow field $\mathbf{u}$ and the pressure field p are governed by the Stokes equation for incompressible fluids [5]:

$$\mu \nabla^2 \mathbf{u} = \nabla p$$

μ is the viscosity of the fluid. Let the fluid domain be bounded by a surface S. Imposing no-slip boundary condition at S leads to the following integral equation [ref] for the three components of the stress density f_k:

$$-U_i(\mathbf{y}) = \frac{3}{2\pi} \int_s \frac{(x_i - y_i)(x_j - y_j)(x_k - y_k) n_j(\mathbf{x}) U_k(\mathbf{x})}{r_{xy}^5} d\mathbf{S}_x + \frac{1}{4\pi} \int_s \left[\frac{\delta_{ij}}{r_{xy}} + \frac{(x_i - y_i)(x_j - y_j)}{r_{xy}^3} \right] f_j(\mathbf{x})\, d\mathbf{S}_x, \ y \in S$$

The repeated indices are consistent with Einstein summation and the first integral requires computation of a Cauchy principle-value integral and the second integral represents the free space Green's function integrated over the particle surface to obtain the net stress density. Upon discretization of S into N triangular elements, a $3N \times 3N$ system is obtained after enforcing no-slip boundary conditions at the surface. The stress densities are obtained by solving this system of equations. The total viscous drag force can then be obtained by integrating the stress densities over the particle surface, $F_D = \int_s f_j\, dS_j$. The force thus obtained can be used to simulate particle motion due to combined DEP and fluidic force fields.

4. Simulation results

Figure 4.1 depicts the electric field produced by a quad phase planar array 10 µm in width, 50 µm in length, spaced at 10-60 µm from each other. Figures 4.2-4.3 depict the circuit topology and the DEP force fields of a four arm spiral array [6]. The outer radius is 6 µm, spiral width 1 µm, and spacing between arms 1 µm. The quad-phase voltage source is operated at 1 MHZ, and is phase shifted by 90^0 between its neighbors to produce traveling wave characteristics. Figure 4.4 depicts the DEP force distribution on spherical and non-spherical micro-particles, with the total force ratio of 1:4. Figure 4.5 shows the fluidic stress distribution on a 10 μm spherical particle and a total drag of $18.6\times10^{-8}\ N$.

References:

[1] Figeys D, Pinto D, *Lab-on-chip: A Revolution in Biological and Medical Sciences*, Ana. Chemistry, May (2000), pp. 330A - 335A.

[2] Haibo, L., Z. Yanan, A. Demir, and R. Bashir, *Characterization and Modeling of Microfluidic Dielectrophoresis Filter for Biological Species*, Journal of MEMS, Vol. 14 No. 1 (2005).

[3] Y. Wang, D. Gope, V. Jandhyala and C.J. Shi, Generalized *KVL-KCL Formulation for Coupled Electromagnetic-Circuit Simulation with Surface Integral Equations*, IEEE Trans. MTT, vol. 52, no. 7, pp. 1673-1682, July 2004.

[4] Chakraborty S, Rockway J, Jandhyala v, *A computational circuit-electromagnetic framework for force prediction on explicitly modeled nanoparticle surfaces in a lab-on-chip environment* APS Symposium, 2005, Volume 1A, 3-8 July 2005, 55 - 58 Vol. 1A.

[5] Pozrikidis C, Introduction to Theoretical and Computational Fluid Dynamics, Oxford University Press, 1997.

[6] Gascoyne P. R., Vykoukal, DEP based Sample Handling in General Purpose Programmable Diagnostic Instruments, Proc IEEE, vol 92, no. 1, 2004, 22-42.

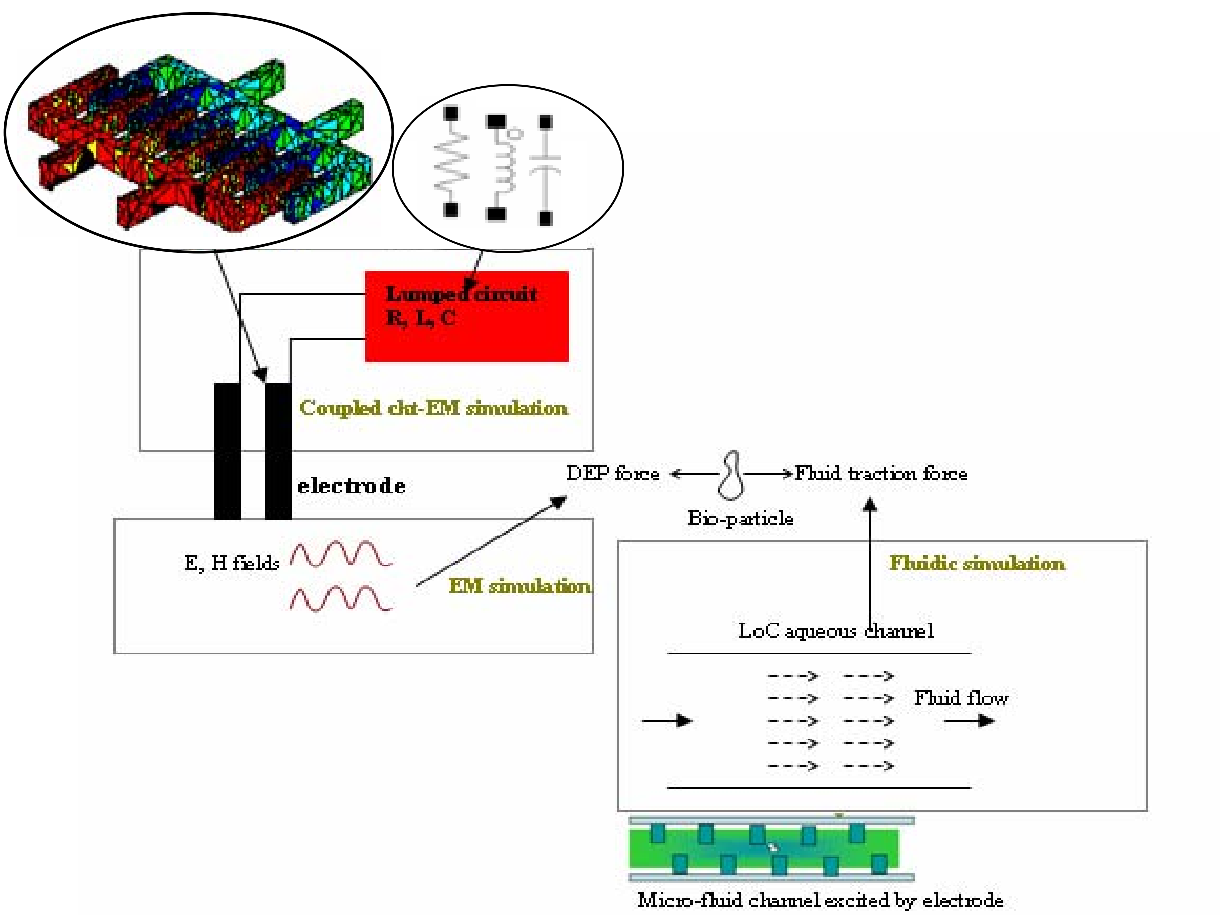

Figure 1: Schematic depicting sources and effects of different forces in a LoC environment

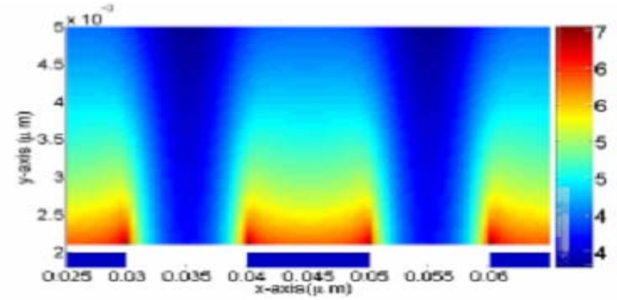

Figure 4.1

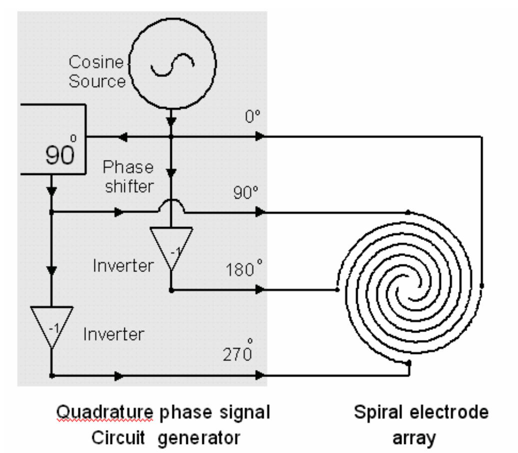

Figure 4.2 [6]

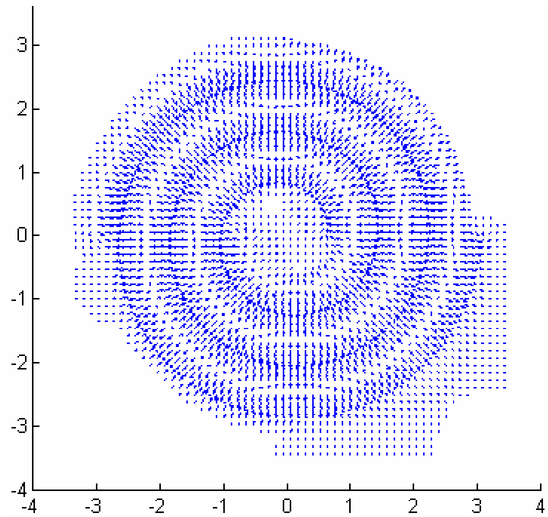

Figure 4.3

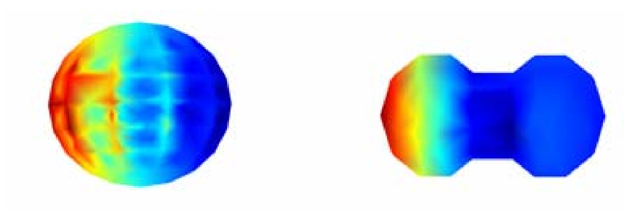

Figure 4.4

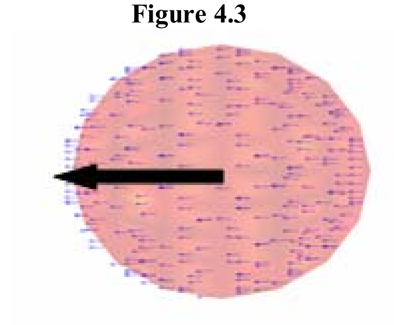

Figure 4.5